California Polytechnic State University

Aerospace Engineering Department

San Luis Obispo, CA

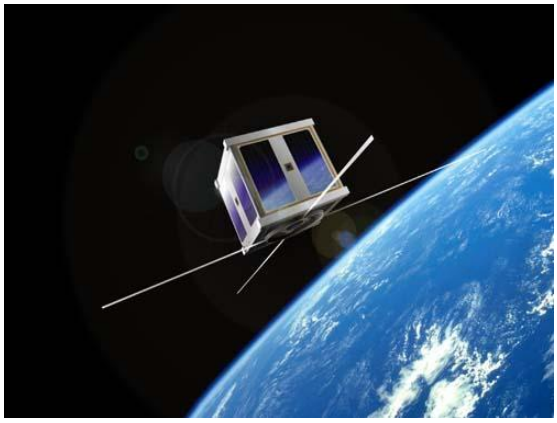

Senior Project

Thermal Analysis of the CubeSat CP3 Satellite

Jonas Friedel and Sean McKibbon

6/7/2011

Due to inconsistencies found in the on-orbit thermal data from the CubeSat CP3 satellite between 2007 and 2011, further analysis is performed on a larger number of data from August 2010 through April 2011, aiming to find an explanation for the overall increasing measured temperatures and shortening peak periods. Therefore, the satellite power data as well as orbital anomalies are analyzed leading to the conclusion that the satellite was temporarily (January – March 2011) orbiting with significantly increased sun exposure causing the higher temperatures. The shortened temperature peak periods are explained by alternating albedo values as the main influence in temperature changes. Typical thermal coefficients for anodized aluminum of the non-solar cell area of the spacecraft are found by performing basic thermal calculations using the critical temperature data.

Table of Contents

1 Introduction 2
2 CP3 temperature data evaluation 2
2.1 Initial comparison of 2007 and 2011 temperature data 2
2.2 Further investigation of 2010 and 2011 temperature data 3
3 Power data analysis 11
3.1 Internal component voltage analysis 11
3.2 Solar panel voltage analysis 12
4 Explaining the temperature data development 14
4.1 Influence of satellite orbit 14
4.2 Influence of albedo values 14
4.3 Influence of thermal coefficients 15
4.4 Potential explanation for data anomalies 15
5 Conclusion 18
Sources 19
Table of Figures 19
Table of Tables 19
Appendix 20

1 Introduction

CP3 is a 10 cm cubic satellite built at Cal Poly San Luis Obispo and was launched on April 17th, 2007. It was launched into an orbit with an inclination of 97.9 degrees and a period of 99.14 minutes. Using the collected temperature and power data, valuable information can be obtained about the health status and the orbital characteristics of the satellite. Once the satellite is on orbit, this information is the only index for explanations when it comes to anomalies of the received data.

2 CP3 temperature data evaluation

2.1 Initial comparison of 2007 and 2011 temperature data

Figures 2.1.1 and 2.1.2 below, show external side temperatures of the CP3 spacecraft that were measured in 2007 and 2011, respectively.

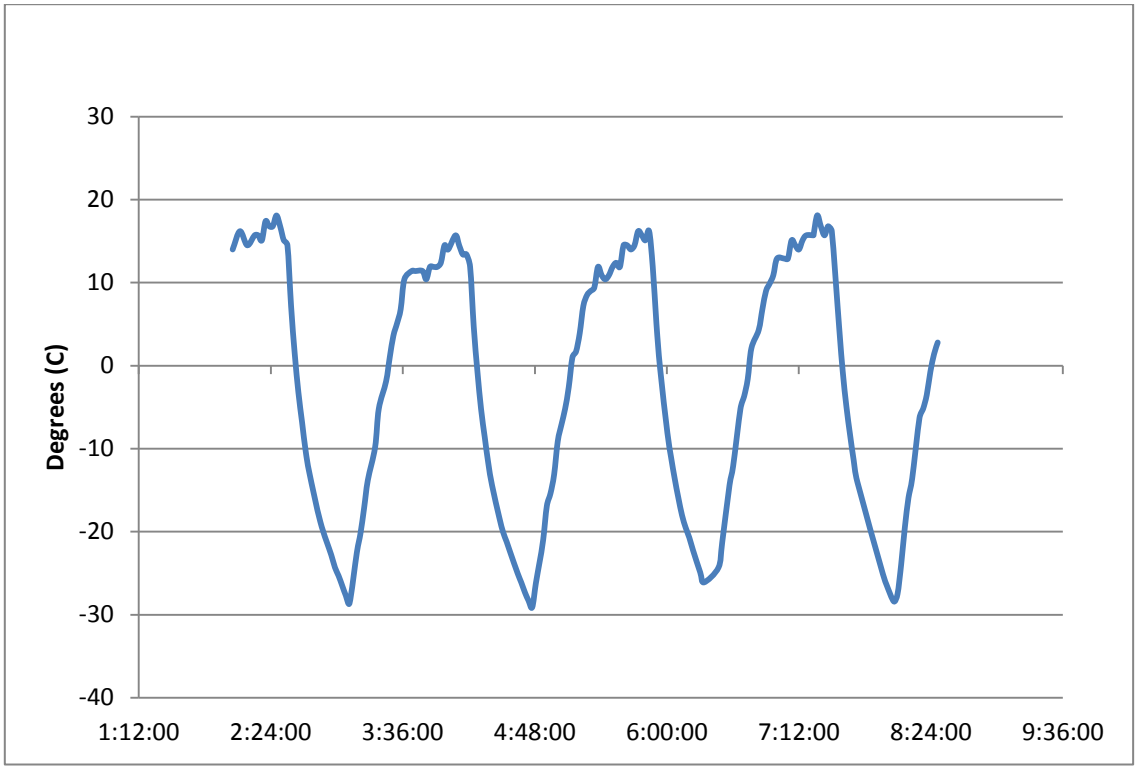

Figure 2.1.1 CP3 external side (JP5) temperatures from 2007

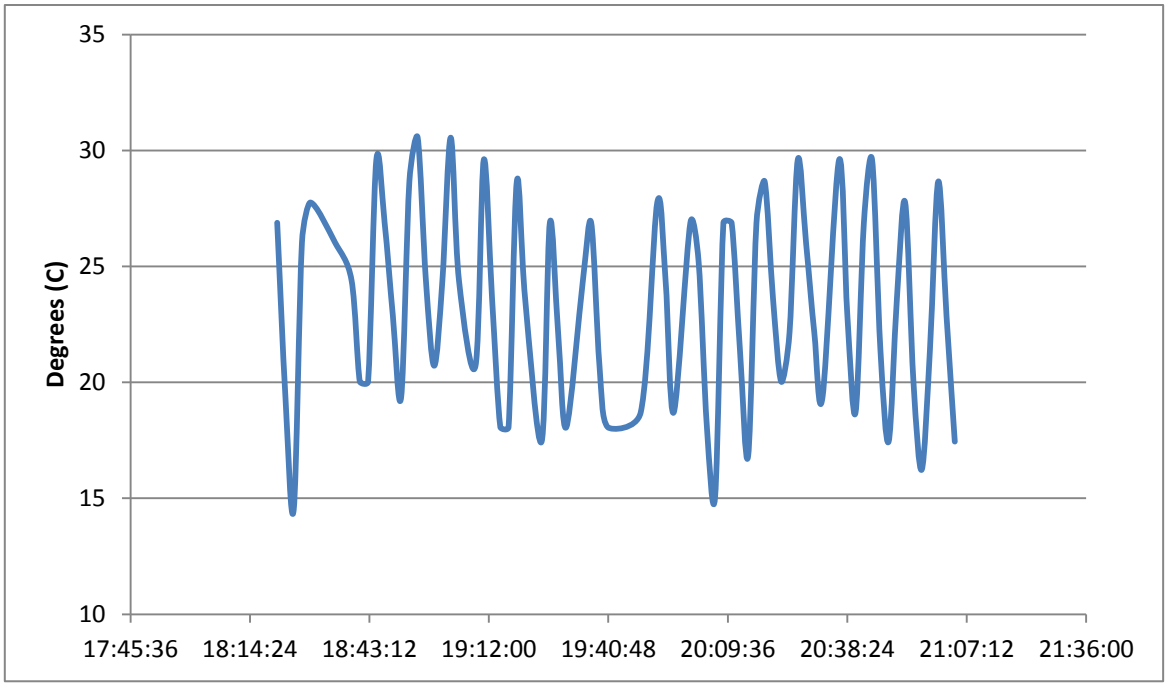

Figure 2.1.2 CP3 external side (JP5) temperatures from 2011

In Figure 2.1.1, the temperature peaks are roughly 90 minutes apart which is what is expected for a satellite in a low Earth orbit. The pattern is the same for all the other temperatures on the other sides of the spacecraft, both internal and external. Plots for each of the individual sides have been created and analyzed from the thermal data to ensure there are no significant differences between each side.

In 2011, however, as it can be seen in figure 2.1.2, the pattern is completely different. The temperature data was taken over a time span of about 7 hours and never drops below 10 degrees C. It does, however, reach peaks of more than 30 degrees in intervals of about 10 to 15 minutes, as compared to the previous 90 minute intervals.

This abnormality required further research and analysis of the thermal data in order to determine the reasons behind those significant changes.

2.2 Further investigation of 2010 and 2011 temperature data

Figures 2.2.1 through 2.2.12 below show the measured external and internal side temperatures of the JP7 side of the satellite, as well as the battery temperatures of selected data dumps from 08/18/2010 through 04/12/2011.

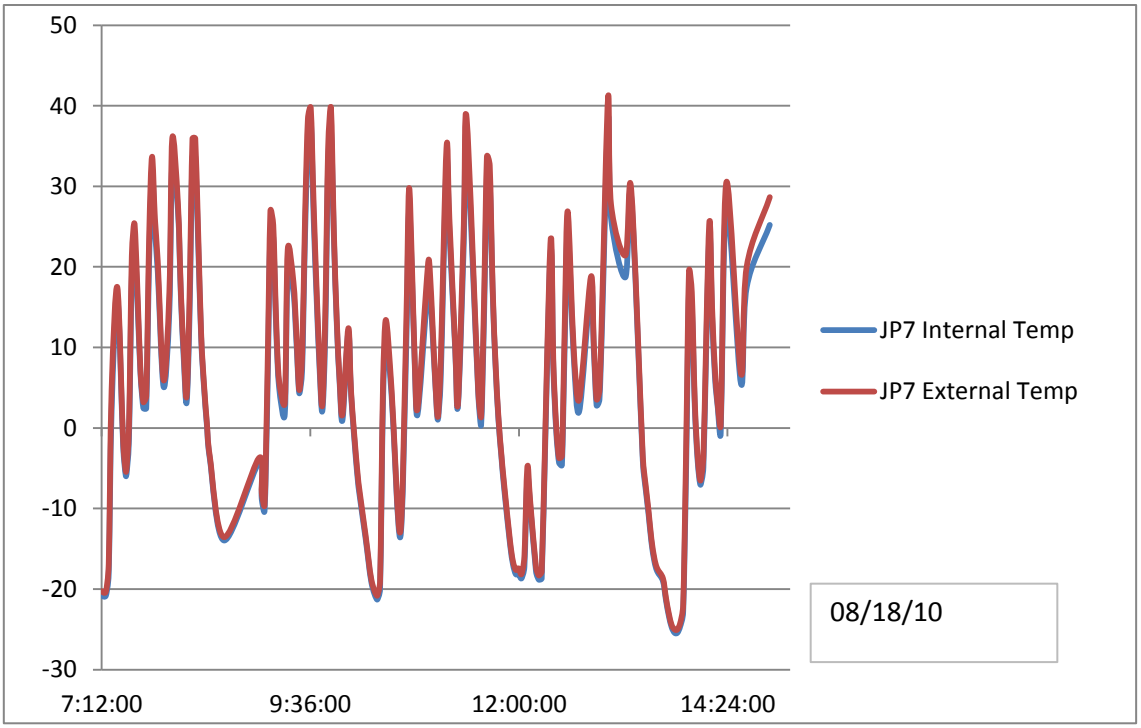

Figure 2.2.1 CP3 side temperatures measured on 08/18/2010

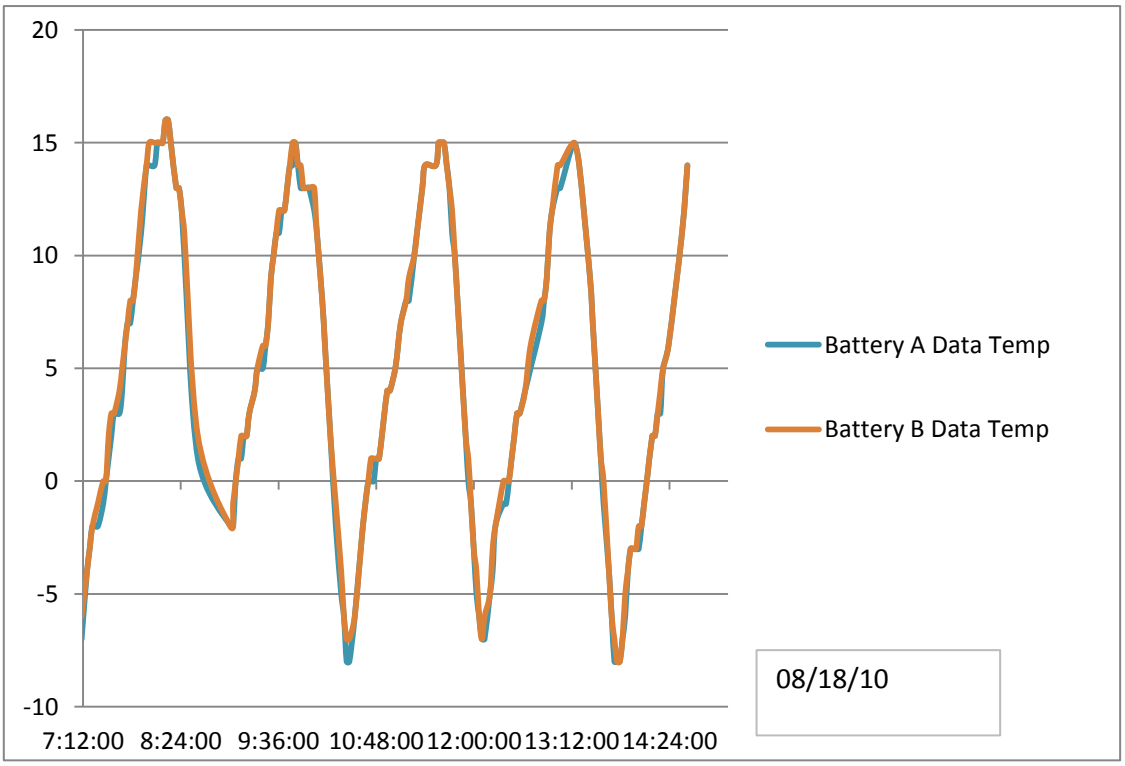

Figure 2.2.2 CP3 battery temperatures measured on 08/18/2010

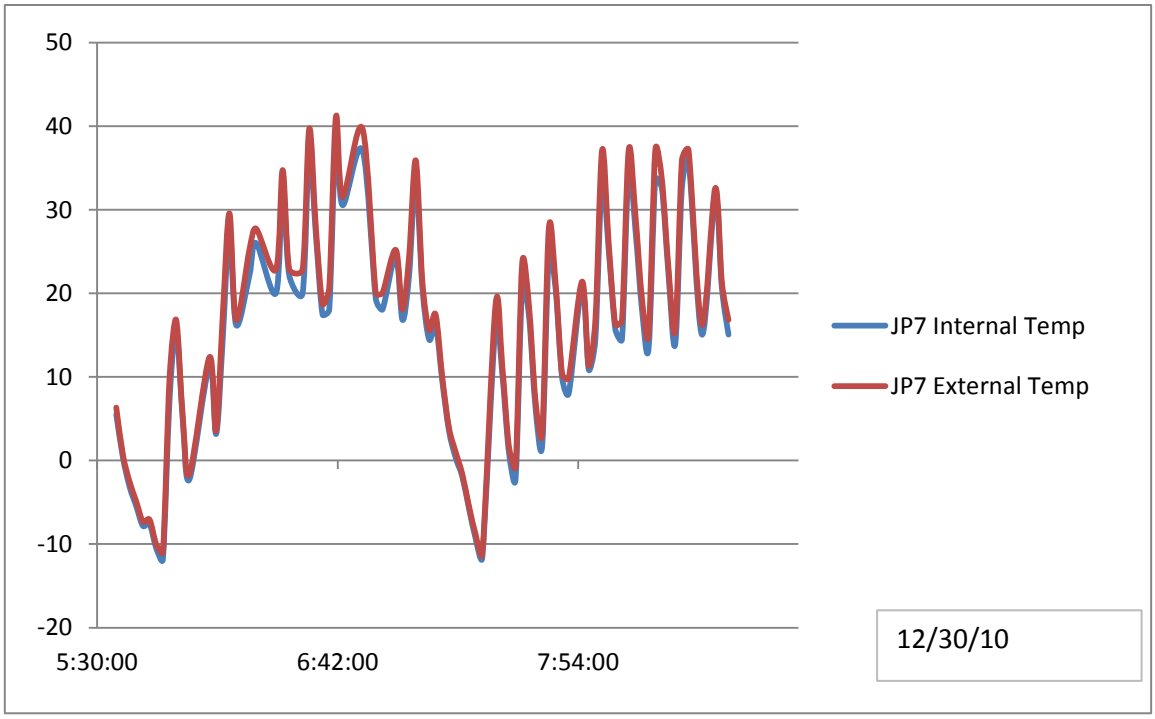

Figure 2.2.3 CP3 side temperatures measured on 12/30/2010

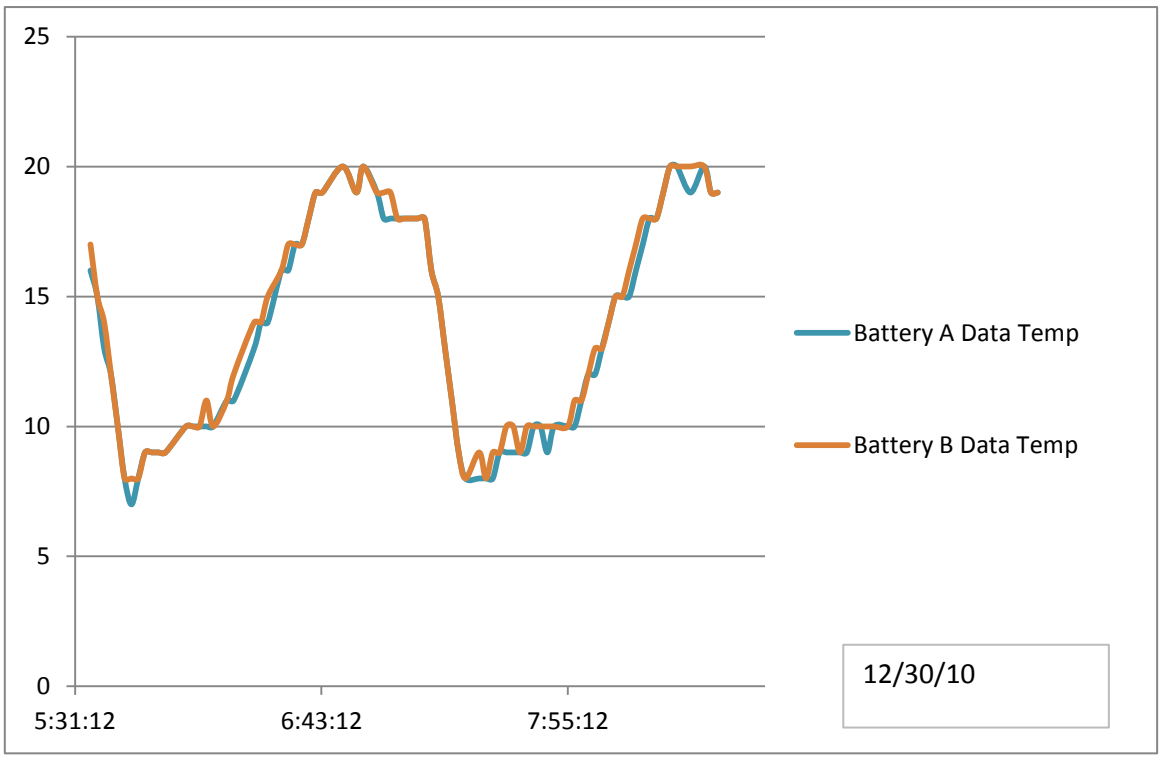

Figure 2.2.4 CP3 battery temperatures measured on 12/30/2010

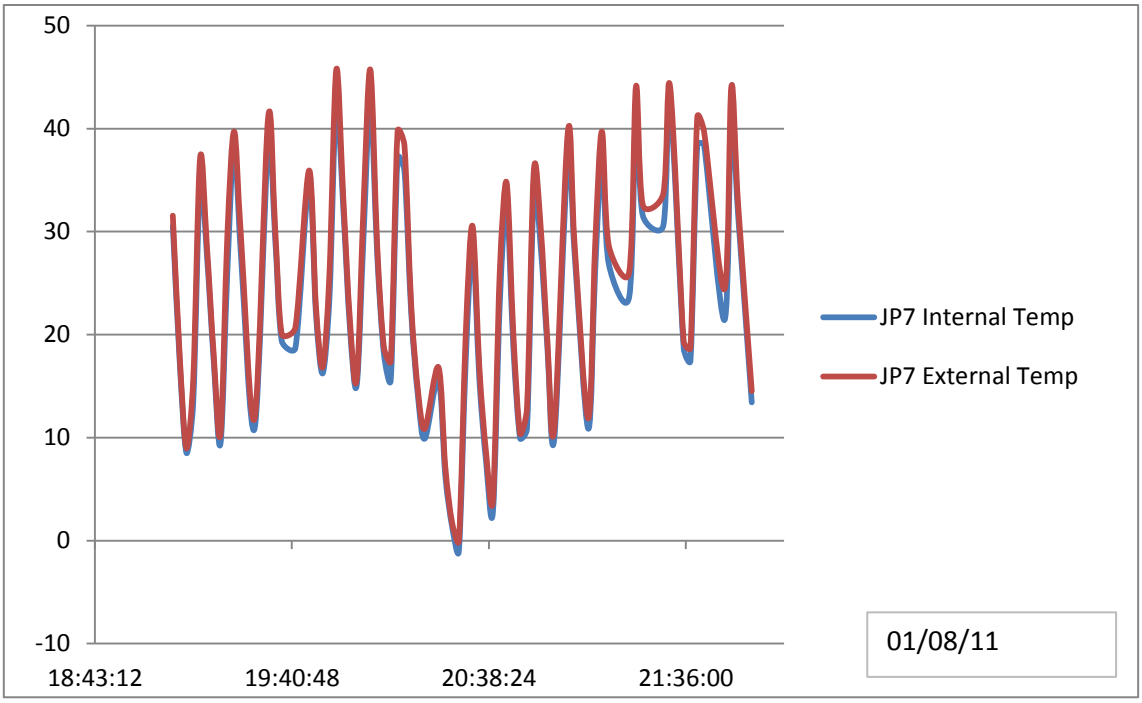

Figure 2.2.5 CP3 side temperatures measured on 01/08/2011

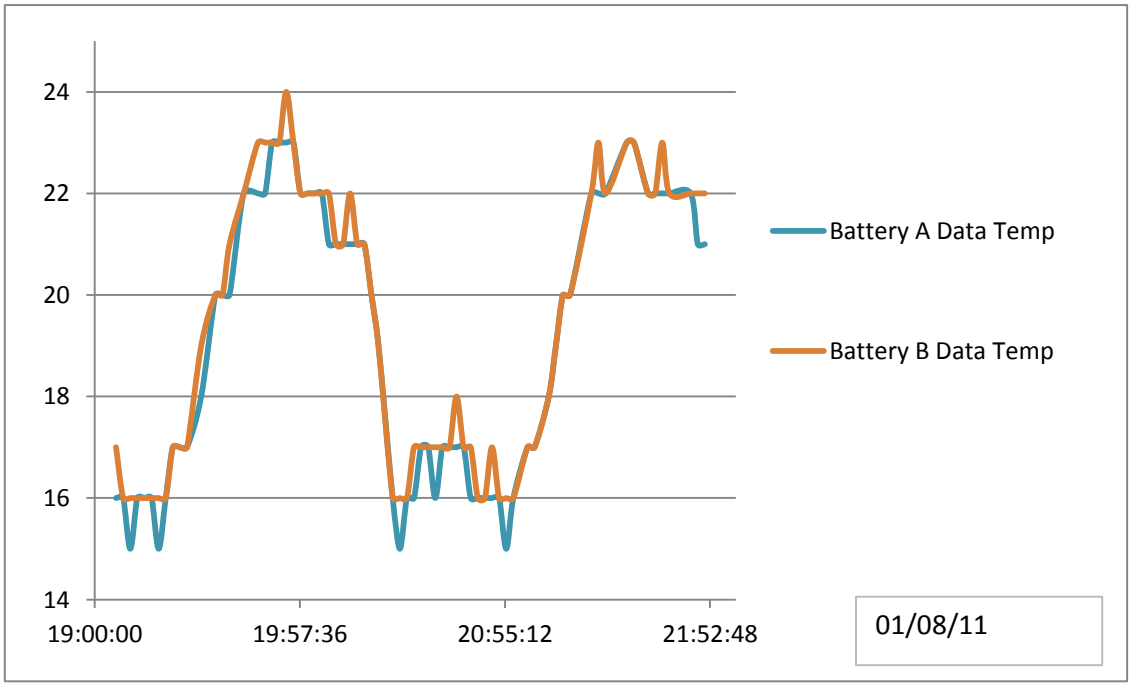

Figure 2.2.6 CP3 battery temperatures measured on 01/08/2011

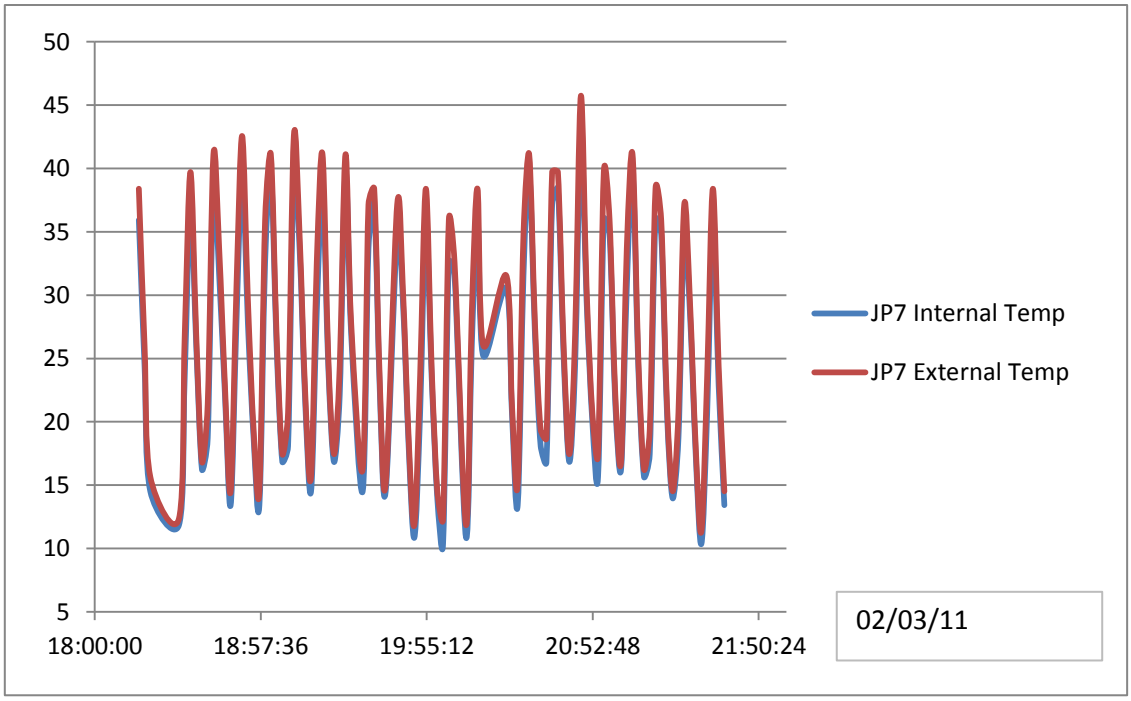

Figure 2.2.7 CP3 side temperatures measured on 02/03/2011

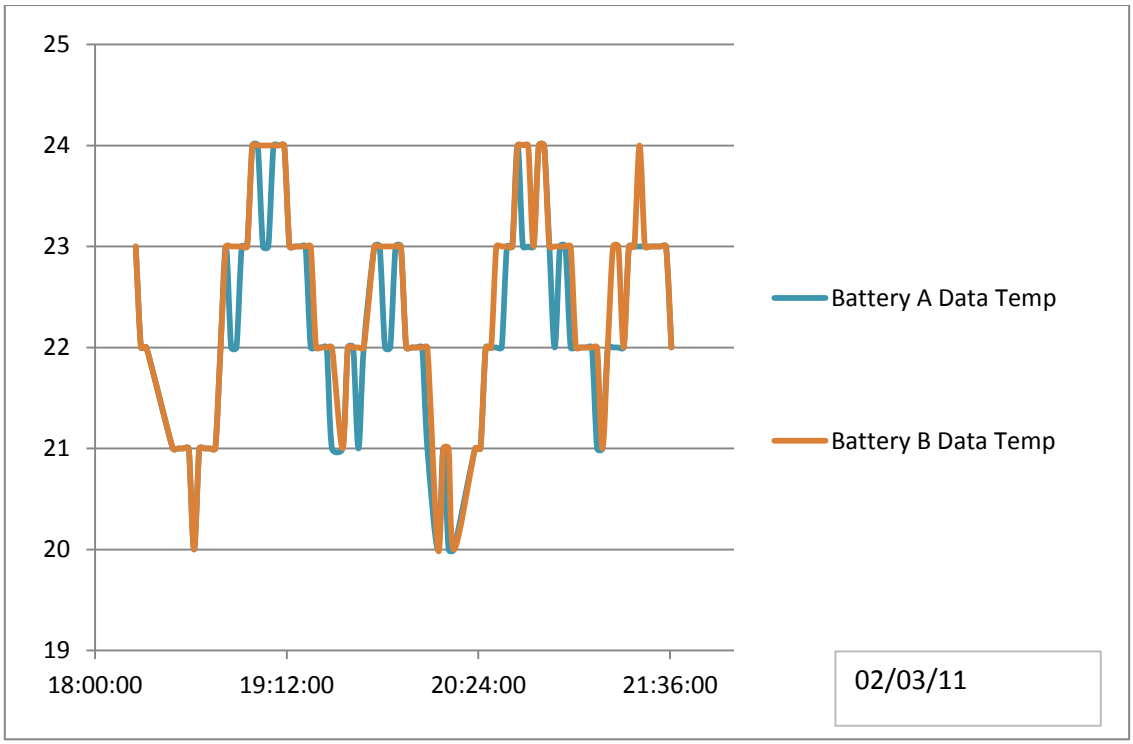

Figure 2.2.8 CP3 battery temperatures measured on 02/03/2011

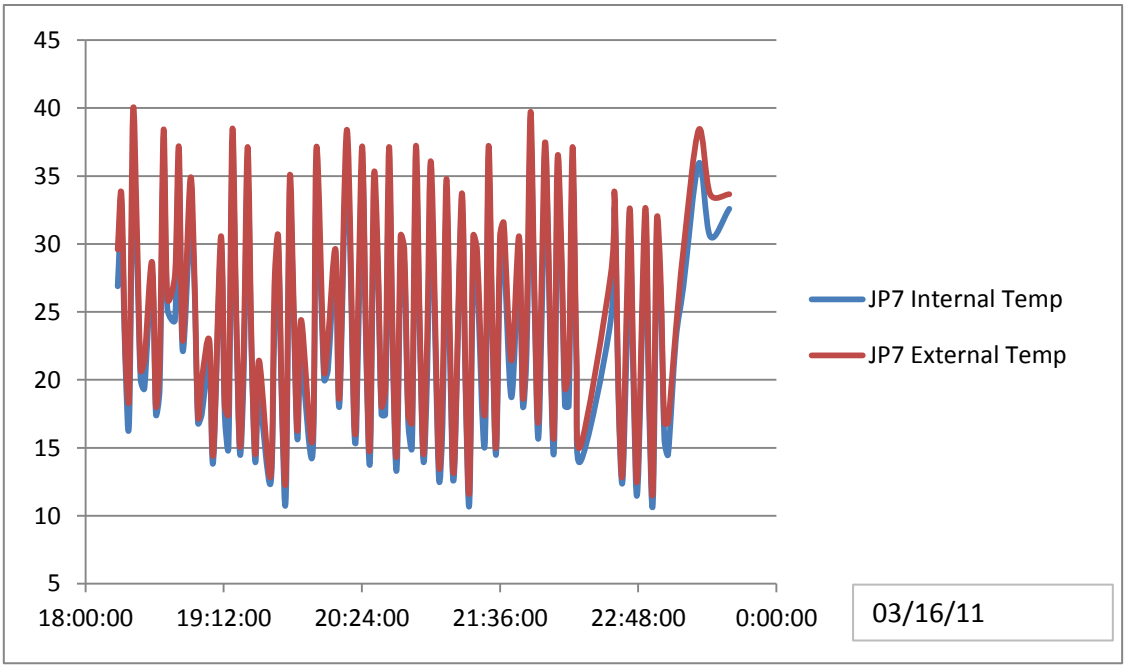

Figure 2.2.9 CP3 side temperatures measured on 03/16/2011

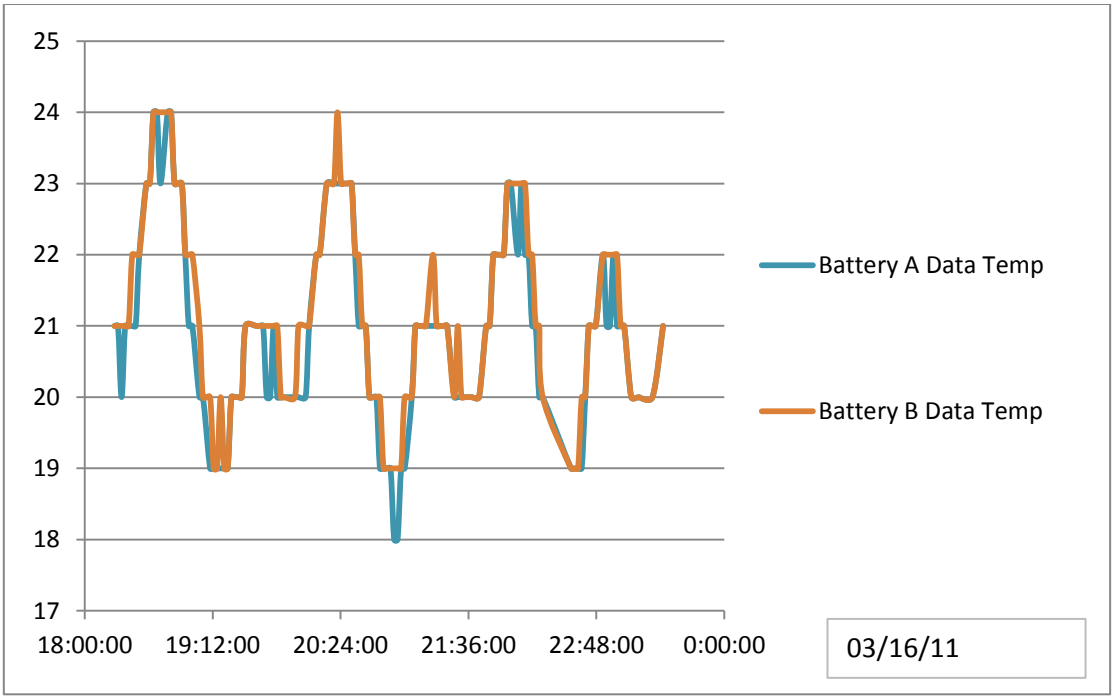

Figure 2.2.10 CP3 battery temperatures measured on 03/16/2011

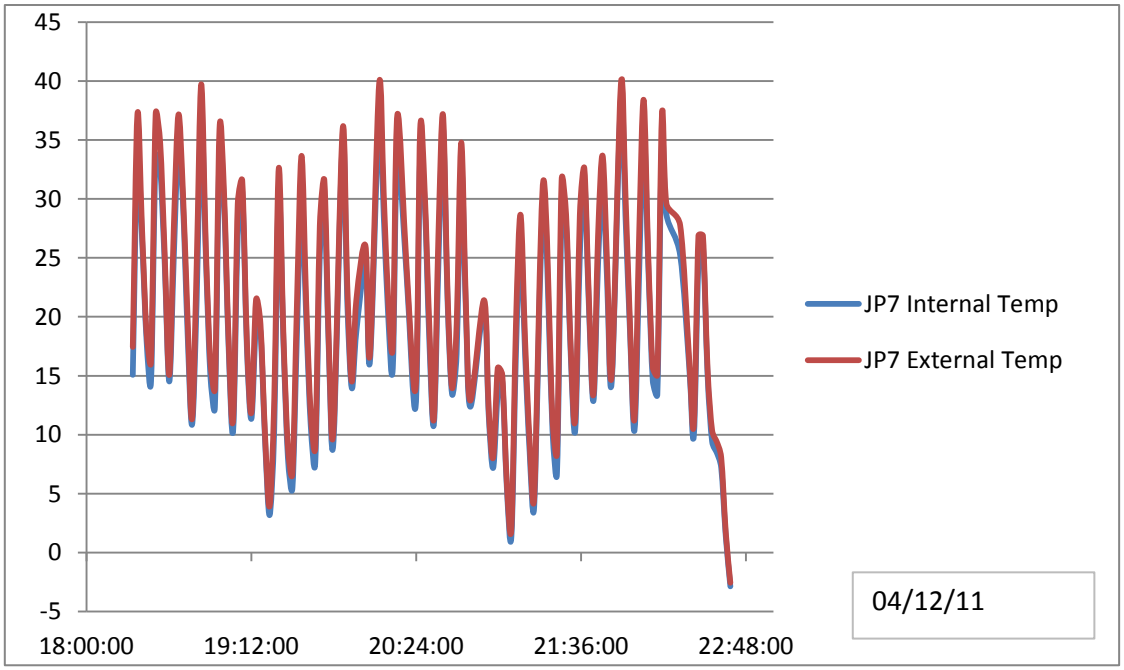

Figure 2.2.11 CP3 side temperatures measured on 04/12/2011

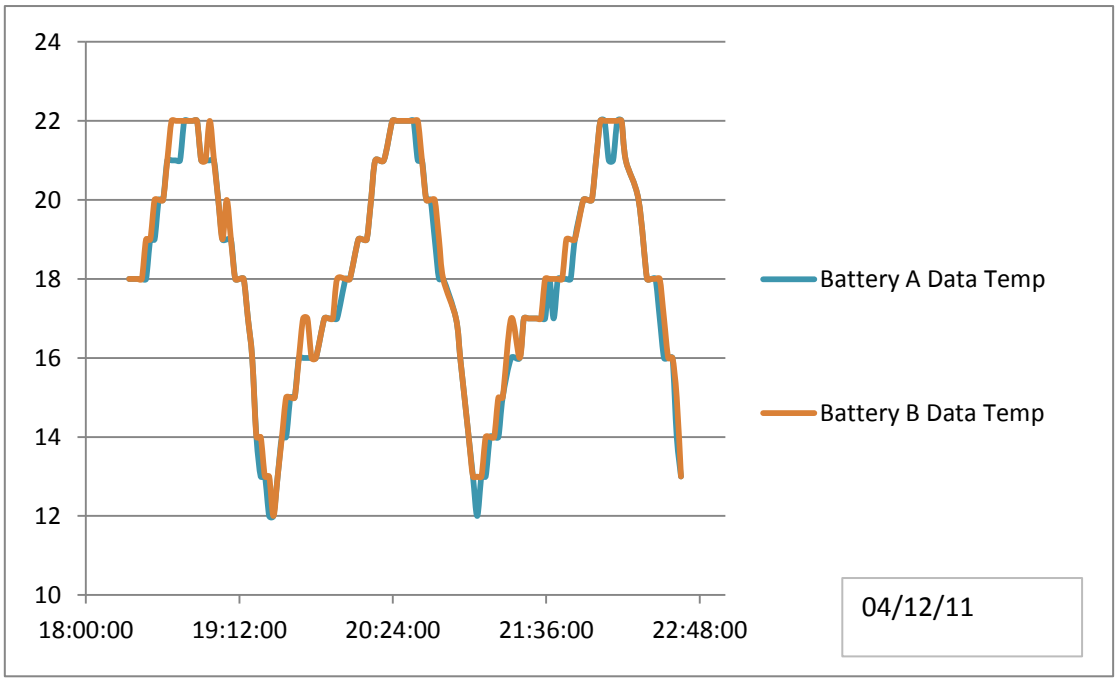

Figure 2.2.12 CP3 battery temperatures measured on 04/12/2011

The figures above show a steady increase in temperature of the satellite and also make the unexpected changes in the temperature peak period very noticeable. While there is a an overall trend of increasing temperatures throughout the considered time span, the most significant change appears on the first data dump of the year 2011 on January 8, when the temperature period shortens and the measured side temperatures never drop below 0 degree C anymore.

Table 2.2.13 below shows a more comprehensive overview of the development of measured temperatures and time periods between the temperature peaks from August 2010 through April 2011. Shown below are both a steady decrease in the temperature range between the maximum and minimum temperatures of the sides of the spacecraft as well as a steady and concerning increase of the minimum temperature of the internal components. Along with these values, and possibly most alarming of all, are the periods observed January through April 2011. The following 8 dumps during that time span provided estimated periods between 35 and 60 minutes which is rather concerning given the expected period of 99.14 minutes. These decreasing time periods between the temperature peaks of the figures raised concern about the current orbit of the spacecraft.

The maximum temperatures of the internal components also steadily rose over the considered time period, but the increase from 20 to 28 degrees was not as significant as the rise of the minimum temperatures from -10 to 22 degrees. This increase prompted new analysis of the internal components and their power data to check for possible failures and the possibility of overheating or malfunction.

Interestingly, for the final data dump, the minimum temperature of the internal components dropped back to 12 degrees and the minimum temperature of the spacecraft sides returned to a negative value of about -7.6 degrees. This could be hinting towards a return to more expected values. However, the period still remains abnormal at about 45-55 minutes. Further research of the most recent data dumps is necessary to determine if the thermal data of the spacecraft does indeed follow this trend.

Table 2.2.1 Temperatures of CP3 sides and internal components with temperature peak periods

	Spacecraft Sides			Internal Components		
date	**max temp**	**min temp**	**temp range**	**max temp**	**min temp**	**period**
18-Aug	45.72601	-27.3978	73.123819	20	-10	90
19-Aug	45.72601	-26.0944	71.8204211	20	-10	90
6-Sep	42.566191	-22.5475	65.1137211	20	-8	90
16-Sep	42.566191	-23.1456	65.7118294	20	-7	90
18-Sep	42.566191	-23.1456	65.7118294	20	-7	90
19-Sep	44.102191	-24.588	68.6902256	21	-7	90
20-Sep	41.108995	-22.8482	63.9571534	20	-6	90
21-Sep	45.72601	-22.8482	68.5741684	21	-5	90
23-Sep	47.4483	-24.0198	71.4681338	23	-6	90
27-Sep	44.102191	-21.4695	65.5717407	22	-5	90
29-Sep	44.102191	-22.396	66.4982062	22	-5	90
1-Oct	44.102191	-21.1539	65.2560809	22	-4	90
3-Oct	41.108995	-20.8347	61.9436778	20	-4	90
9-Oct	41.108995	-21.1539	62.2628844	22	-3	90
10-Oct	42.566191	-21.7817	64.3479311	23	-3	90
11-Oct	44.102191	-22.2437	66.3458783	22	-3	90
22-Oct	45.72601	-20.6737	66.3997344	23	-2	90
3-Nov	44.102191	-20.9947	65.0969259	21	0	90

13-Dec	44.102191	-20.8347	64.9368743	22	-1	90
14-Dec	44.102191	-18.319	62.4211528	22	0	90
15-Dec	41.108995	-20.9947	62.1037295	22	-1	90
16-Dec	39.722911	-20.6737	60.3966352	22	0	90
21-Dec	44.102191	-16.1326	60.2347596	23	2	90
24-Dec	41.108995	-19.5207	60.6297284	23	2	90
26-Dec	41.108995	-18.8402	59.9492386	23	3	90
28-Dec	42.566191	-13.349	55.9152246	23	5	90
30-Dec	41.108995	-14.9729	56.0818473	23	6	90
8-Jan	47.4483	-5.45341	52.9017121	25	15	45-50
14-Jan	44.102191	2.082984	42.0192072	28	20	45-55
28-Jan	45.72601	3.559113	42.1668969	28	20	?
1-Feb	45.72601	1.024138	44.7018723	28	20	50-60
3-Feb	45.72601	2.811462	42.9145477	27	21	50-55
5-Feb	47.4483	2.082984	45.3653162	27	22	35-45
7-Feb	47.4483	2.811462	44.6368381	27	22	45-50
2-Mar	44.102191	1.024138	43.0780537	27	20	50
14-Mar	42.566191	0.339548	42.2266426	27	20	50-55
16-Mar	47.4483	1.024138	46.4241626	27	20	45-60
12-Apr	47.4483	-7.57845	55.0267466	26	12	45-55

3 Power data analysis

3.1 Internal component voltage analysis

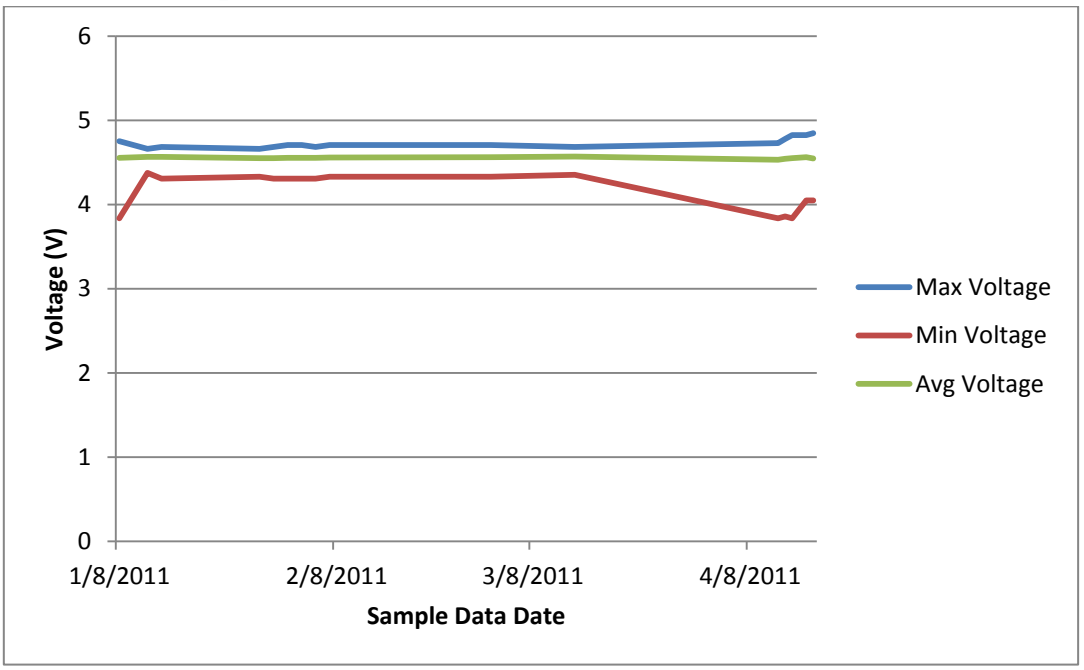

Figure 3.1.1 CP3 CDH VSUM Voltage Data

After considering a possible electronic failure, investigation of power data was necessary. The next step was to obtain, interpret, and analyze this information from the internal components. The first to be examined was the command & data handling VSUM voltage data, shown in Figure 3.1.1 above, which covers the time span of the abnormal thermal periods (January 8th through April 12th). Overall, the voltages remained constant and do not show any indication that this is the cause of the increase in temperature of the internal components. The maximum, minimum, and average voltages are all plotted and none of them deviate much from 4.5 Volts indicating that there is no malfunction in this region of the satellite. The minimum voltages dip off a little around April 2011 and could possibly explain the drop from 20 to 12 degrees of the internal components in Table 2.2.1, but to justify this, further analysis needs to be done on the most recent data dumps.

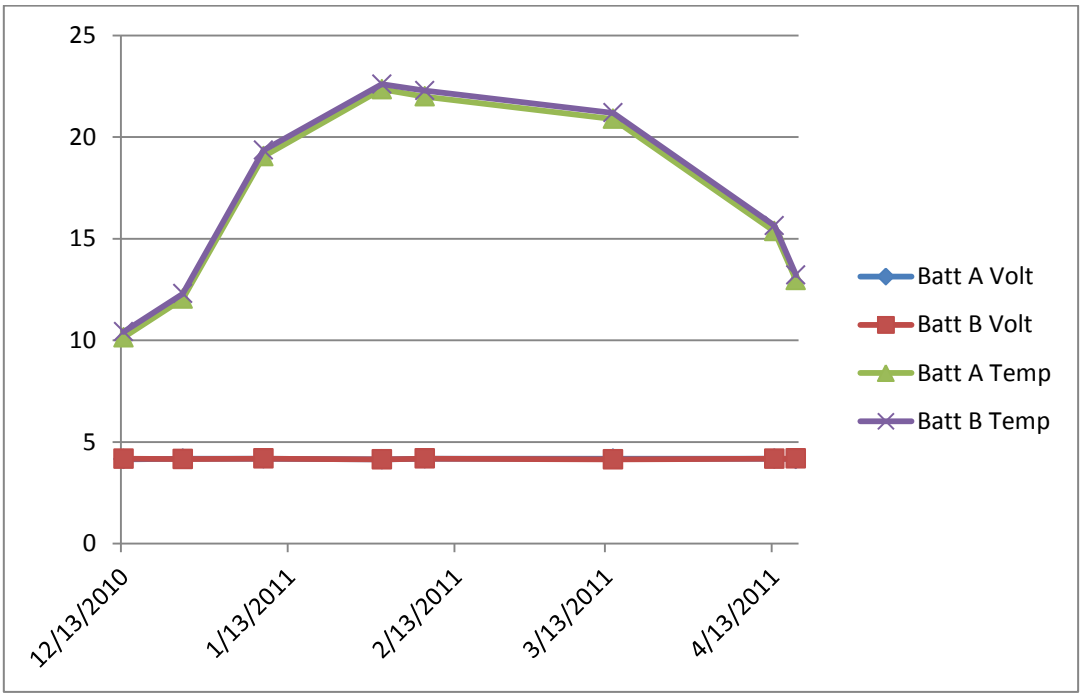

Figure 3.1.2 Battery voltages and temperatures from January 8 to April 12, 2011

After seeing that the VSUM data did not indicate any malfunctions, the next step was to analyze the temperatures and voltages of the batteries. Figure 3.1.2 above shows both, the voltages and temperatures of batteries A and B within the satellite over the time period of interest. Very similar to the aforementioned VSUM data, the battery temperatures remain around a constant 4 Volts. The temperatures, however, do follow the temperature pattern of the satellite sides as shown in table 2.2.1 under the internal components column. This indicates that a possible voltage leak, as thought to be a possibility for the temperature increase, was not the cause. Another hypothesis was that the batteries were overloaded with power from the solar panels and were releasing the excess energy as heat, thus causing the spacecraft to warm up.

3.2 Solar panel voltage analysis

As it was unknown whether the increase of temperatures throughout the spacecraft were caused by overheating components, defect thermostats or an actual increase in sun exposure, the measurements of the solar panels voltages were examined since they display a voltage of around 5 Volts when exposed to the sun and 0 Volts when not exposed to the sun. For this examination, the measurements of the side JP7 were used because this side showed values that were representative

of all the other sides. The thought behind this examination was that if the satellite was to be in an orbit that causes it to see the sun more often than in previous cases, the solar panels would more often measure a higher frequency of 5 Volts as opposed to 0 Volts and, therefore, produce a higher average number of voltages measured. As it can be seen in figure 3.2.1 below, the average values of the measured solar panel voltage increase significantly in 2011, supporting the assumption that the satellite experiences a higher exposure to the sun than in 2010.

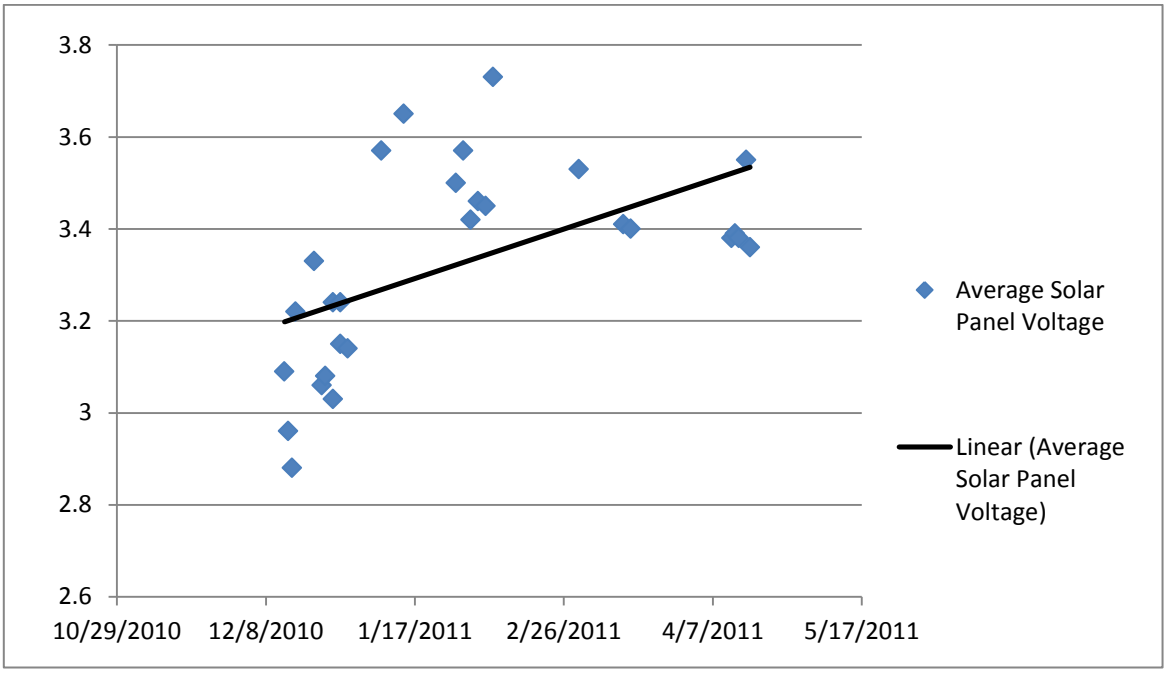

Figure 3.2.1 Average solar panel voltage (JP7) over time

To further support this assumption, the solar panel voltages were compared to the side temperatures of the satellite, which can be seen in figures 3.2.2 and 3.2.3 below.

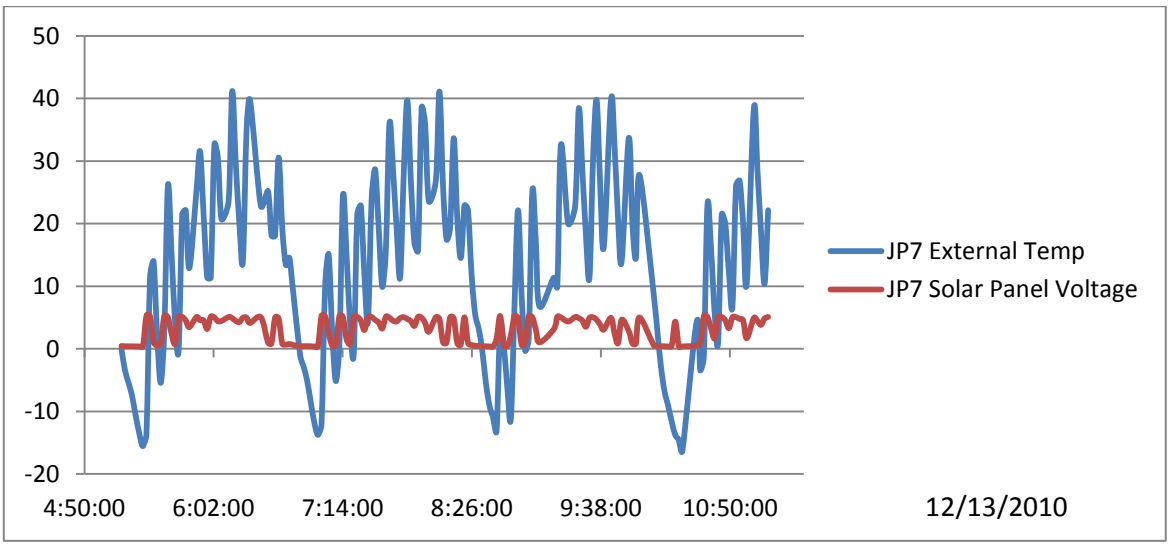

Figure 3.2.2 Comparison of temperatures and solar panel voltages from 12/13/2010

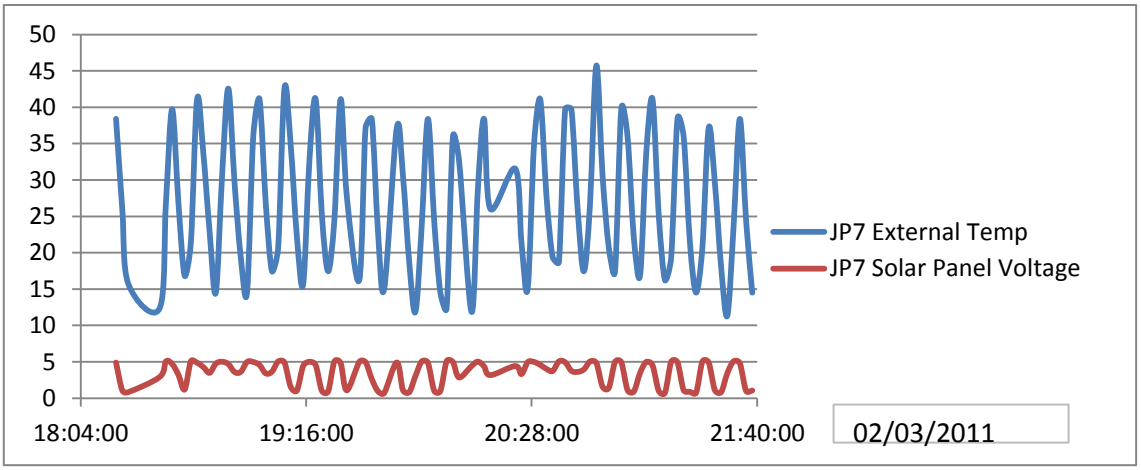

Figure 3.2.3 Comparison of temperatures and solar panel voltages from 02/03/2010

As expected, the solar panel voltages follow the same trend as the temperature values. This can be explained by the fact that both, the temperatures and solar panel voltages are dependent on the input from the sun, which causes higher temperatures and produces voltage in the panels. The observation that, despite changing temperature patterns between figure 3.2.2 (December 2010) and 3.2.3 (February 2011), the solar panel voltage values still follow the pattern of the temperatures, indicating again that the increasing temperature are likely to be caused by the satellite spending an increased amount of time in the sun.

4 Explaining the temperature data development

4.1 Influence of satellite orbit

According to the satellite orbit information on www.space-track.org and the information received from the CubeSat team, the satellite is still in its regular orbit with an inclination of 97.9 degrees and has a period of 99.14 minutes. However, it is assumed that the satellite is flying in an orbit that would cause it to constantly see the sun during the time of the data irregularities (January – March 2011). As shown in section 3.2 above, the satellite indeed seems to receive an increased sun input during that time which supports the orbit assumption. This would explain the rising temperatures measured on the CubeSat. Figure 4.1.1 below shows a schematic of the assumed satellite orbit.

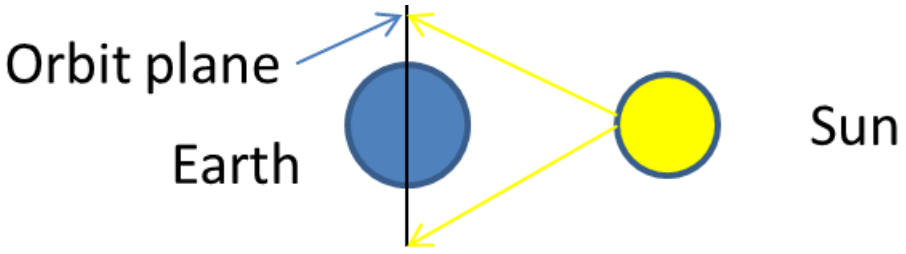

Figure 4.1.1 Satellite orbit with constant sun exposure

4.2 Influence of albedo values

If the satellite was in an orbit that would constantly see the sun, the difference of the solar flux between different phases of a single period would be eliminated. Therefore, the albedo influence

would present the dominating factor in creating temperature differences during each rotation period. The albedo differences would be caused by the satellite passing over different latitudes of the earth, with higher latitudes generally causing a higher albedo factor than lower latitudes due to increased cloud and ice coverage. Since the albedo is sun light reflected back from the Earth to the spacecraft, it is measured in percent of the solar flux and is very variable. Table 4.2.1 below shows some typical average albedo values for various Earth orbits.

Table 4.2.1 Albedo values for various orbit (SMAD, 433)

Orbit inclination (deg)	Angle of sun out of orbit plane (deg)	Albedo (percent)	
		Min. Value	**Max. value**
0-30	0	18	28
	90	45	55
30-60	0	23	30
	90	50	57
60-90	0	23	30
	90	50	57

Since the satellite is in a 99.14 degree inclination, the albedo values from the high inclinations (60 - 90 degrees) would be used in this case. If, as assumed in section 4.1, the satellite was in an orbit that constantly sees the sun, the nature of the angle between such an orbit and the sun vector would cause the spacecraft to experience rather low albedo influences.

4.3 Influence of thermal coefficients

To understand the influence of the thermal coefficients on the spacecraft temperature, one must look at the geometry of the CubeSat satellite first. Each side of the cube-shaped satellite has an area of 100cm^2, where each side is covered with two solar panels covering a total area of 42 cm^2. The remaining area of each side is mostly made of anodized aluminum. While the thermal coefficients of the solar panel area can be estimated to be 0.825 for emissivity and 0.805 for absorptivity, the thermal coefficients for the remaining area are unknown. Knowing the temperatures measured on orbit and using basic thermal calculations, the influence of different thermal coefficients of the remaining side areas could be used as an aid to explain the abnormal temperature data.

4.4 Potential explanation for data anomalies

To understand this approach, it is important to know that it is not the main objective of this examination to find the exact albedo values and thermal coefficients that match the temperature data. The following calculations were performed to find out whether the discovered abnormal temperature behaviors can be explained using the assumptions made and the factors considered in this section.

For this calculation, the satellite was considered to be in an orbit that causes it to constantly see the sun, while permanently being exposed to a constant solar flux, relatively low but alternating albedo influences and a constant Earth radiation (IR). The solar flux was assumed to be the solar constant (1376 W/m^2), the IR was assumed to be 231 W/m^2, which is an average value for high orbit inclinations. (SMAD, 433) As described in section 4.3 above, the side area of the cubic satellite is 100cm^2, where 42% of the area is covered with solar panels that have an emissivity if 0.825 and an absorptivity of 0.805 while the thermal coefficients of the remaining area are unknown. For the calculations, a constant internal heat dissipation of 0.323 Watt was used. (CubeSat)

Using the energy equilibrium of equal incoming and outgoing heat, the outgoing heat (Q_{out}) is solely influenced by the radiation through all the six side areas, while the incoming heat (Q_{in}) is divided up into the components of solar, IR and albedo influence, as well as the internal dissipation. It is also assumed that the entire external heat energy input (solar, IR and albedo) is received through the projected area of one spacecraft side facing the Earth. Here is an overview of the equations used for the thermal calculations,

Equation 4.4.1

$$Q_{in} = Q_{out}$$

Equation 4.4.2

$$Q_{out} = 6A\sigma\varepsilon T^4$$

Equation 4.4.3

$$Q_{in} = Q_{solar} + Q_{IR} + Q_{albedo} + Q_{internal}$$

Equation 4.4.4

$$Q_{solar} = G_{solar}(A_{solar\ panel}\alpha_{solar\ panel} + A_{rest}\alpha_{rest})$$

Equation 4.4.5

$$Q_{IR} = G_{IR}(A_{solar\ panel}\varepsilon_{solar\ panel} + A_{rest}\varepsilon_{rest})$$

Equation 4.4.6

$$Q_{albedo} = G_{albedo}(A_{solar\ panel}\alpha_{solar\ panel} + A_{rest}\alpha_{rest})$$

where A is the side area of the satellite (100 cm^2), σ is Stefan Boltzmann's constant (5.670×10^{-8} W/m^2K^4), ε is the emissivity, α the absorptivity, T the temperature (K) and G is the heat flux (W/m^2).

To eliminate the unknown factor of the satellite's tumbling rate, the battery temperatures were considered for this calculation as they are located in the center of the spacecraft and do not experience temperature variations through orientation changes of the satellite. As it can be seen in section 2.2.1, the battery temperatures during the critical period (January – March 2011) usually range between 20 and 24 degree C. As explained in section 4.2 above, the albedo values from high inclinations were used for this calculation. Also, the satellite being in an orbit that constantly sees the sun results in low albedo reflections from the Earth, which is why the minimum albedo values at high orbit inclinations are used ($albedo_{min}$=23%, $albedo_{max}$=30%). Figures 4.4.1 and 4.4.2 below show the calculated satellite temperatures for the maximum and minimum considered albedo value of 30% and 23%, respectively, of the solar flux depending on the emissivity and absorptivity of the non-solar cell area of the spacecraft sides.

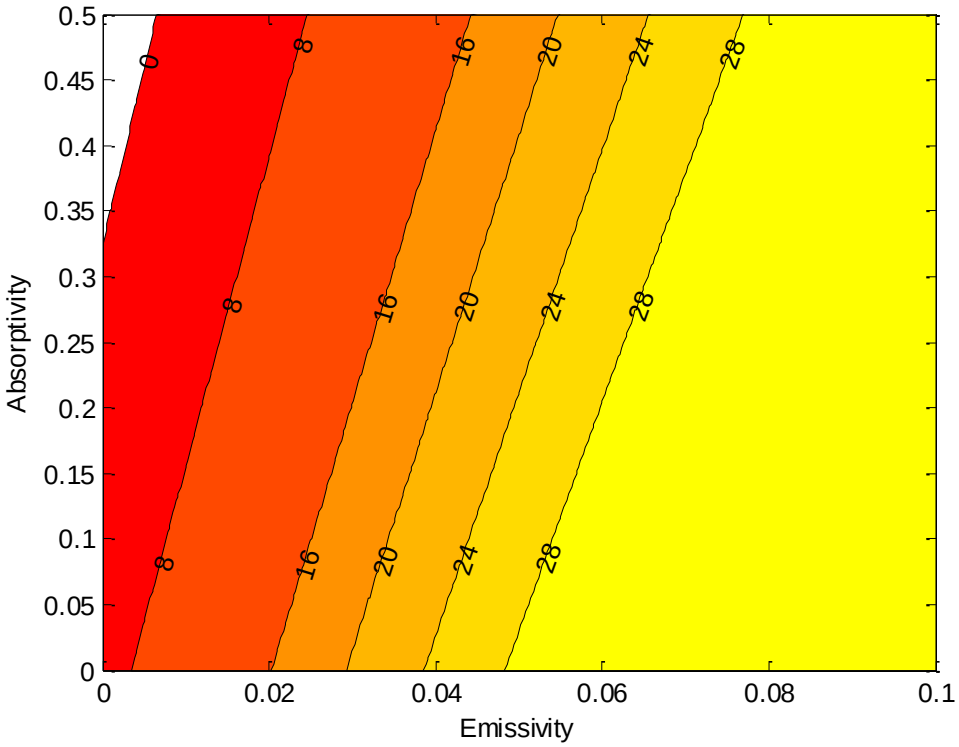

Figure 4.4.1 Theoretical satellite temperatures at maximum albedo of 30%

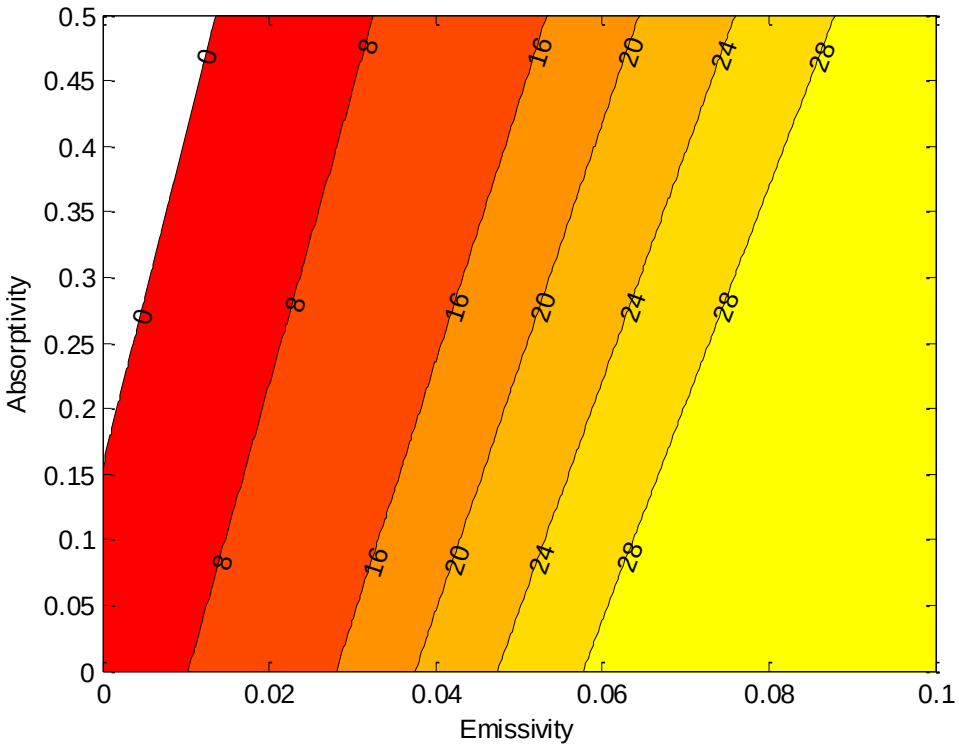

Figure 4.4.2 Theoretical satellite temperatures at maximum albedo of 23%

Looking at the figures above, one can get a rough idea of what kind of emissivity and absorptivity values of the non-solar cell area are theoretically required to achieve the measured spacecraft

battery temperatures of 20 and 24 degree C, respectively. Table 4.4.1 below shows a selection of calculated temperature values based on the thermal coefficients shown above.

Table 4.4.1 Calculated temperatures at selected emissivity and absorptivity values

Absorptivity	Emissivity	Temperature at min. albedo (23%) in deg C	Temperature at min. albedo (30%) in deg C
0.25	0.040	20.7	24.3
0.25	0.045	20.1	23.7
0.25	0.050	19.6	23.2

The key information in table 4.4.1 above is that at an absorptivity of 0.25 at emissivity values between 0.040 and 0.050 can cause temperature differences between the maximum and minimum considered albedo values of about 3.5 degree C, where the actual measured difference lies at about 4 degree C. Also, for the thermal coefficients shown in the table, the calculated temperatures are in the range of about 20 to 24 degree C, which are the minimum and maximum temperatures that were actually measured in the batteries (see section 2.1.1). The thermal coefficients used in the table are typical for anodized aluminum, which happens to be the material that was actually used for most of the non-solar cell area of the spacecraft. (CubeSat)

Therefore, it can be concluded that when bringing together all the assumptions, the abnormal temperature patterns that were measured from January through April 2011 can be explained with the satellite flying in an orbit with no eclipses, in which the only temperature variations are caused by alternating albedo values. The changes in the albedo values are caused by the spacecraft passing over higher and lower latitudes of the Earth. This also explains the shortened temperature periods that were discussed in section 2.2.2.

5 Conclusion

The most important take away from this investigation is that the temperature behavior of the CP3 spacecraft can be explained when taking a closer look at the circumstances, such as the orbital constellation and thermal properties of the material, and is not due to component overheating, as it was assumed at first. Obviously, the assumptions that were made and the calculations that were performed only allowed for a conceptual investigation rather than a detailed analysis. However, it was important for CubeSat to know that their first ever satellite in orbit is not in the process of overheating, which is valuable information for future products and the space qualification of the components that were used. A more detailed analysis of the thermal behavior of the CubeSat satellites can be achieved by determining the thermal properties of the materials through vacuum chamber tests and by obtaining more information on the thermal influences on the satellite, such as solar flux and albedo at the respective orbital position.

Sources

- CubeSat
- James R. Wertz, W. J. (2009). *Sapce Mission Analysis and Design (SMAD).* Microcosm Press.

Table of Figures

Figure 2.1.1 CP3 external side (JP5) temperatures from 2007 2
Figure 2.1.2 CP3 external side (JP5) temperatures from 2011 3
Figure 2.2.1 CP3 side temperatures measured on 08/18/2010 4
Figure 2.2.2 CP3 battery temperatures measured on 08/18/2010 4
Figure 2.2.3 CP3 side temperatures measured on 12/30/2010 5
Figure 2.2.4 CP3 battery temperatures measured on 12/30/2010 5
Figure 2.2.5 CP3 side temperatures measured on 01/08/2011 6
Figure 2.2.6 CP3 battery temperatures measured on 01/08/2011 6
Figure 2.2.7 CP3 side temperatures measured on 02/03/2011 7
Figure 2.2.8 CP3 battery temperatures measured on 02/03/2011 7
Figure 2.2.9 CP3 side temperatures measured on 03/16/2011 8
Figure 2.2.10 CP3 battery temperatures measured on 03/16/2011 8
Figure 2.2.11 CP3 side temperatures measured on 04/12/2011 9
Figure 2.2.12 CP3 battery temperatures measured on 04/12/2011 9
Figure 3.1.1 CP3 CDH VSUM Voltage Data 11
Figure 3.1.2 Battery voltages and temperatures from January 8 to April 12, 2011 12
Figure 3.2.1 Average solar panel voltage (JP7) over time 13
Figure 4.1.1 Satellite orbit with constant sun exposure 14
Figure 4.4.1 Theoretical satellite temperatures at maximum albedo of 30% 17
Figure 4.4.2 Theoretical satellite temperatures at maximum albedo of 23% 17

Table of Tables

Table 2.2.1 Temperatures of CP3 sides and internal components with temperature peak periods 10
Table 4.2.1 Albedo values for various orbit (SMAD, 433) 15
Table 4.4.1 Calculated temperatures at selected emissivity and absorptivity values 18

Appendix

Matlab Code

```
%%orbit inclination=97.9 deg (source: space-track)
%Q_in (W/m^2)
G_sun=1376;
G_sun_ecl=0;
G_IR=(218+244)/2; %average value
%% Albedo values
% Average min albedo
G_alb_min=0.23*G_sun; %(0.23+0.50)/2*G_sun;
% Average max albedo
G_alb_max=0.30*G_sun; %(0.30+0.57)/2*G_sun;
% Eclipse albedo
G_alb_ecl=0;
%%
% side dimensions (m^2)
%full spacecraft side
A=0.1^2;
%solar cell area per side
A_sc=2*0.03*0.07;
%remaining area per side
A_rest=A-A_sc;
%internal dissipation (W)
Q_int=0.323;
%Boltamann constant
boltz=5.67e-8; %W/(m^2*K^4)
%% emissitvity/absorptivity values of materials
%solar cells
em_sc=0.825;
abs_sc=0.805;
%aluminum (bare)
em_al=linspace(0.03,0.10,10);
abs_al=linspace(0.09,0.17,10);
%aluminum (anodized)
```

```
%em_al_an=linspace(0.04,0.88,20);

%abs_al_an=linspace(0.25,0.86,20);

%black paint (chemglaze)

em_bp_chem=linspace(0.89,0.89,10);

abs_bp_chem=linspace(0.92,0.98,10);

%black paint (3M black velvet)

em_bp_3M=linspace(0.84,0.84,10);

abs_bp_3M=linspace(0.97,0.97,10);

%white paint (chemglaze)

em_wp_chem=linspace(0.88,0.88,10);

abs_wp_chem=linspace(0.22,0.28,10);

%Test

em_test=linspace(0,0.1,101);

abs_test=linspace(0,0.5,101);

%% Temperature claculation

for i=1:length(em_test);

   for j=1:length(abs_test);


%T_al_min(i)=(((A_sc*abs_sc+A_rest*abs_al(i))*G_sun+(A_sc*em_sc+A_rest*em_al(i))*G_IR+(A_sc*abs_sc+A_rest*abs_al(i))*G_alb_min+
Q_int)/(6*(A_sc*em_sc+A_rest*em_al(i))*boltz))^(1/4)-273;


%T_al_max(i)=(((A_sc*abs_sc+A_rest*abs_al(i))*G_sun+(A_sc*em_sc+A_rest*em_al(i))*G_IR+(A_sc*abs_sc+A_rest*abs_al(i))*G_alb_max
+Q_int)/(6*(A_sc*em_sc+A_rest*em_al(i))*boltz))^(1/4)-273;


%T_al_an_min(j)=(((A_sc*abs_sc+A_rest*abs_al_an(j))*G_sun+(A_sc*em_sc+A_rest*em_al_an(j))*G_IR+(A_sc*abs_sc+A_rest*abs_al_an(j
))*G_alb_min+Q_int)/(6*(A_sc*em_sc+A_rest*em_al_an(j))*boltz))^(1/4)-273;


%T_al_an_max(j)=(((A_sc*abs_sc+A_rest*abs_al_an(j))*G_sun+(A_sc*em_sc+A_rest*em_al_an(j))*G_IR+(A_sc*abs_sc+A_rest*abs_al_an(j
))*G_alb_max+Q_int)/(6*(A_sc*em_sc+A_rest*em_al_an(j))*boltz))^(1/4)-273;


%T_bp_chem_min(i)=(((A_sc*abs_sc+A_rest*abs_bp_chem(i))*G_sun+(A_sc*em_sc+A_rest*em_bp_chem(i))*G_IR+(A_sc*abs_sc+A_rest*
abs_bp_chem(i))*G_alb_min+Q_int)/(6*(A_sc*em_sc+A_rest*em_bp_chem(i))*boltz))^(1/4)-273;


%T_bp_chem_max(i)=(((A_sc*abs_sc+A_rest*abs_bp_chem(i))*G_sun+(A_sc*em_sc+A_rest*em_bp_chem(i))*G_IR+(A_sc*abs_sc+A_rest
*abs_bp_chem(i))*G_alb_max+Q_int)/(6*(A_sc*em_sc+A_rest*em_bp_chem(i))*boltz))^(1/4)-273;


%T_bp_3M_min(i)=(((A_sc*abs_sc+A_rest*abs_bp_3M(i))*G_sun+(A_sc*em_sc+A_rest*em_bp_3M(i))*G_IR+(A_sc*abs_sc+A_rest*abs_b
p_3M(i))*G_alb_min+Q_int)/(6*(A_sc*em_sc+A_rest*em_bp_3M(i))*boltz))^(1/4)-273;


%T_bp_3M_max(i)=(((A_sc*abs_sc+A_rest*abs_bp_3M(i))*G_sun+(A_sc*em_sc+A_rest*em_bp_3M(i))*G_IR+(A_sc*abs_sc+A_rest*abs_b
p_3M(i))*G_alb_max+Q_int)/(6*(A_sc*em_sc+A_rest*em_bp_3M(i))*boltz))^(1/4)-273;


%T_wp_chem_min(i)=(((A_sc*abs_sc+A_rest*abs_wp_chem(i))*G_sun+(A_sc*em_sc+A_rest*em_wp_chem(i))*G_IR+(A_sc*abs_sc+A_rest
*abs_wp_chem(i))*G_alb_min+Q_int)/(6*(A_sc*em_sc+A_rest*em_wp_chem(i))*boltz))^(1/4)-273;
```

```
%T_wp_chem_max(i)=(((A_sc*abs_sc+A_rest*abs_wp_chem(i))*G_sun+(A_sc*em_sc+A_rest*em_wp_chem(i))*G_IR+(A_sc*abs_sc+A_rest*abs_wp_chem(i))*G_alb_max+Q_int)/(6*(A_sc*em_sc+A_rest*em_wp_chem(i))*boltz))^(1/4)-273;

T_test_min(i,j)=(((A_sc*abs_sc+A_rest*abs_test(j))*G_sun+(A_sc*em_sc+A_rest*em_test(i))*G_IR+(A_sc*abs_sc+A_rest*abs_test(j))*G_alb_min+Q_int)/(6*(A_sc*em_sc+A_rest*em_test(i))*boltz))^(1/4)-273;

T_test_max(i,j)=(((A_sc*abs_sc+A_rest*abs_test(j))*G_sun+(A_sc*em_sc+A_rest*em_test(i))*G_IR+(A_sc*abs_sc+A_rest*abs_test(j))*G_alb_max+Q_int)/(6*(A_sc*em_sc+A_rest*em_test(i))*boltz))^(1/4)-273;

T_test_eclipse(i,j)=(((A_sc*abs_sc+A_rest*abs_test(j))*G_sun_ecl+(A_sc*em_sc+A_rest*em_test(i))*G_IR+(A_sc*abs_sc+A_rest*abs_test(j))*G_alb_ecl+Q_int)/(6*(A_sc*em_sc+A_rest*em_test(i))*boltz))^(1/4)-273;

   T_eclipse(i,j)=(((A_sc*em_sc+A_rest*em_test(i))*G_IR+Q_int)/(6*(A_sc*em_sc+A_rest*em_test(i))*boltz))^(1/4)-273;

   end

end


Max_temp=T_test_max(51,51)

Min_temp=T_test_min(51,51)


[x,y]=meshgrid(em_test,abs_test);

v=[0 8 16 20 24 28];

figure(1)

[C,h]=contourf(x,y,T_test_min,v);

clabel(C,h)

xlabel('Emissivity')

ylabel('Absorptivity')

zlabel('Minimum Temperature')

%title('Minimum Temperature depending on Emissivity and Absoprtivity of Non-solar cell area')

colormap Autumn

[x,y]=meshgrid(em_test,abs_test);

v=[0 8 16 20 24 28];

figure(2)

[C,h]=contourf(x,y,T_test_max,v);

clabel(C,h)

xlabel('Emissivity')

ylabel('Absorptivity')

zlabel('Maximum Temperature')

%title('Maximum Temperature depending on Emissivity and Absoprtivity of Non-solar cell area')

colormap Autumn
```